Available online at www.sciencedirect.com
SCIENCE DIRECT®
Journal of Solid State Chemistry 177 (2004) 2464–2469
JOURNAL OF SOLID STATE CHEMISTRY
http://elsevier.com/locate/jssc

Crystal structure and electrical properties of the mixed valent titanium oxysulfide $Sm_2Ti_2S_2O_{4.5}$

C. Guillot-Deudon,* V. Meignen, L. Cario, A. Lafond, and A. Meerschaut

Department of Chemistry, Laboratoire de Chimie des Solides, 2 rue de la Houssinière, BP 32229 44322 Nantes cedex 03, France

Received 2 March 2004; received in revised form 9 April 2004; accepted 13 April 2004

Abstract

A new phase $Sm_2Ti_2S_2O_{4.5}$ was synthesized and its crystal structure was solved by single-crystal X-ray diffraction. This compound crystallizes in the monoclinic system (*C*2/*m*) with lattice constants $a = 17.9987(11)$ Å, $b = 3.71607(14)$ Å, $c = 12.6172(8)$ Å and $\beta = 133.645(4)^\circ$. The structure is built up from double chains of Ti-centered octahedra between which Sm-polyhedra develop. In spite of very close formulations, the structure of $Sm_2Ti_2S_2O_{4.5}$ differs completely from that of the defect Ruddelsden–Popper phase $Sm_2Ti_2S_2O_5$ previously reported. The title compound presents a mixed valence for titanium with Ti(III) (d^1) and Ti(IV) (d^0) located in different crystallographic sites. However, conductivity measurements show that this compound is non-metallic.

Keywords: Mixed valence; Titanium; Oxysulfide; Rare earth; Crystal structure

1. Introduction

In the past few years, oxychalcogenides have seen a renewed interest with the discovery of compounds that exhibit interesting physical properties (p-type transparent conducting compounds [1], photocatalytic activity [2], etc.) and/or interesting structural features (anionic segregation [3], layered structures [4,5]). Among all systems, the rare-earth titanium oxychalcogenide system has been the most studied and several compounds have been characterized, as exemplified for instance by $La_8Ti_{10}S_{24}O_4$ [6], $La_4Ti_2Se_5O_4$ and $La_6Ti_3Se_9O_5$ [7], $Ln_2Ti_2S_2O_5$ [8], and $Gd_4TiSe_4O_4$ [9]. In most cases, titanium adopts the +IV oxidation state, but it was also found with the +III oxidation state or in a mixed valence state. The ability for Ti cations to present both oxidation states could lead to interesting electronic properties around the metal–insulator transition.

The $Ln_2Ti_2S_2O_5$ compounds, which belong to the Ruddelsden–Popper family, exhibit layered structures based on the stacking of sulfide [Ln_2S_2] and oxide [Ti_2O_5] layers [8]. The oxide layer is of ReO_3 type with empty sites, and contains Ti(IV) cations only. By filling the voids with Cu atoms we have attempted to reduce the Ti atoms planning to induce a metal–insulator transition in these phases; intercalation of alkali metals into these phases has been already performed with success [10]. Our attempt was unsuccessful but we have obtained a new phase $Sm_2Ti_2S_2O_{4.5}$ that contains both Ti(III) and Ti(IV). This paper reports on the structure determination of this compound. A special interest was focused on the characterization of the mixed valence state.

2. Synthesis

In the aim of inserting Cu atoms in the phase $Sm_2Ti_2S_2O_5$, a mixture of this phase with Cu metal was progressively heated to 1000°C in a silica tube during 1 week. Some small ribbon-shaped crystals were found and easily selected from the black powder. Semi-quantitative chemical analyses were carried out using a JEOL 5800 SEM equipped with a PGT EDS-micro-analyzer. The analysis results, averaged over 4 crystals, confirmed the presence of oxygen and agree well with

*Corresponding author. Fax: +33-240-37-39-95.
E-mail address: catherine.deudon@cnrs-imn.fr (C. Guillot-Deudon).

0022-4596/$ - see front matter © 2004 Elsevier Inc. All rights reserved.
doi:10.1016/j.jssc.2004.04.012

the structural composition of $Sm_2Ti_2S_2O_{4.5}$ for non-oxygen atoms (i.e. 33% for each), as follows: Sm: 33.8 at%, Ti: 33.6 at%, S: 32.7 at%. The oxygen content was deduced from the crystal structure determination.

3. Structure determination

A crystal with dimensions $0.010 \times 0.192 \times 0.010\,mm^3$ was mounted on a Kappa CCD diffractometer using Mo$K\alpha$ radiation. The crystal-to-detector distance was set to 30 mm; 281 frames were recorded with a rotation angle of 2° and an exposure time of 200 s per frame. The recorded images were processed with the set of programs from Nonius using the Eval CCD formalism [11]. The symmetry was monoclinic and the resulting cell parameters were: $a = 17.9987(11)$ Å, $b = 3.71607(14)$ Å, $c = 12.6172(8)$ Å and $\beta = 133.645(4)°$. A total of 7232 reflections ($-28<h<28$, $-5<k<5$, $-20<l<20$) were measured over the range $2.23°<\theta<34.98°$. Intensity statistic favored the centrosymmetric space group *C2/m* (no. 12). Data collection details are given in Table 1.

The positions of the heaviest atoms (Sm and Ti) were determined by the direct methods using the SHELX program [12]. Then, sulfur and oxygen atoms were found from subsequent difference Fourier syntheses and least-squares refinements. Refinement on 1500 unique reflections was performed using the JANA 2000 program [13]. The refinement converged to a R(obs) value of 4.78% for 1121 reflections ($I>2\sigma(I)$) corrected from absorption via the faces indexed option. However, at this stage of refinement (i.e. with anisotropic displacement parameters for Sm and Ti but isotropic for S and O), the displacement parameter for one O atom (=O5) was abnormally high (ten times the averaged value for the other O atoms). As this atom was located on a special position (Wyckoff site 2*c*: 0,0, 1/2), we changed its position for a more general one (Wyckoff site 4*m*: *x*,0,*z*, with $x\approx 0$ and $z\approx 1/2$) with a statistical occupancy of 50%. This led to better reliability factors: $R(\text{obs}) = 4.45\%$ and $R_w(\text{obs}) = 5.36\%$, and a thermal displacement parameter for O5 more realistic and comparable to those of the other oxygen atoms. At the last stage of the refinement, with anisotropic displacement parameters

Table 1
Cell parameters, crystallographic data, and refinement results for $Sm_2Ti_2S_2O_{4.5}$

Physical and crystallographic data	
Formula	$Sm_2Ti_2S_2O_{4.5}$
Molar mass ($g\,mol^{-1}$)	532.6
Color	Black
Crystal size (mm^3) boundaries	$0.010 \times 0.192 \times 0.010$ {100},{010},{001}, {30–2}
Space group	*C*2/*m* (no. 12)
Z	4
a (Å)	17.9987(11)
b (Å)	3.71607(14)
c (Å)	12.6172(8)
β	133.645(4)
V(Å^3)	609.21(6)
Calculated density ($g\,cm^{-3}$)	5.805
Absorption coefficient (mm^{-1})	22.147
Recording conditions	
Temperature (K)	293
Radiation λ (Å)	0.71073 (Mo$K\alpha$)
Diffractometer	Nonius CCD
Angular range θ (°)	2.23–34.98
$-h$, $+h$; $-k$, $+k$; $-l$, $+l$ range	−28, 28; −5, 5; −20, 20
Data reduction	
Recorded reflections all; obs ($I>2\sigma(I)$)	1500; 1121
Absorption correction	Gaussian method based on crystal shape
Transmission min–max	0.2039–0.8268
Refinement (based on F)	
No of refined parameters	53
R/R_w (%) on observed reflections ($I>2\sigma(I)$)	3.33/3.40
R/R_w (%) on all reflections	6.65/3.70
Goodness of fit	1.11
Residual electronic density (e^- Å^{-3}) (deapest/highest)	−2.91; +2.63

Table 2
Atomic coordinates and equivalent isotropic displacement parameters for $Sm_2Ti_2S_2O_{4.5}$

Atom	Site	s.o.f.	x	y	z	U_{iso}/U_{eq}[a]
Sm1	4*i*	1	0.13674(3)	0	0.82825(4)	0.0055(2)[a]
Sm2	4*i*	1	0.34090(3)	$\frac{1}{2}$	0.68707(4)	0.0057(2)[a]
Ti1	4*i*	1	0.06517(10)	$\frac{1}{2}$	0.96547(15)	0.0043(7)[a]
Ti2	4*i*	1	0.11787(12)	0	0.5380(2)	0.0145(9)[a]
S1	4*i*	1	0.04148(15)	$\frac{1}{2}$	0.3404(2)	0.0415(2)[a]
S2	4*i*	1	0.1998(2)	$\frac{1}{2}$	0.7277(3)	0.020(2)[a]
O1	4*i*	1	0.1775(4)	$\frac{1}{2}$	0.9785(6)	0.005(1)
O2	4*i*	1	0.2339(4)	0	0.5627(6)	0.004(1)
O3	4*i*	1	0.0406(4)	0	0.9098(6)	0.007(1)
O4	4*i*	1	0.4104(4)	0	0.8678(6)	0.0083(11)
O5	4*i*	0.50	0.0215(8)	0	0.5526(12)	0.009(2)

s.o.f. = site occupancy factor.
[a] U_{eq} is defined as one-third of the trace of the orthogonalized U_{ij} tensor.

Table 3
Anisotropic displacement parameters for $Sm_2Ti_2S_2O_{4.5}$

	U_{11}	U_{22}	U_{33}	U_{12}	U_{13}	U_{23}
Sm1	0.0067(2)	0.0029(2)	0.0082(2)	0	0.0056(2)	0
Sm2	0.0079(2)	0.0025(2)	0.0041(2)	0	0.0032(2)	0
Ti1	0.0062(5)	0.0021(6)	0.0058(6)	0	0.0046(5)	0
Ti2	0.0114(6)	0.0229(9)	0.0162(8)	0	0.0123(6)	0
S1	0.0060(8)	0.0037(8)	0.012(1)	0	0.0025(7)	0
S2	0.0489(2)	0.0043(9)	0.0328(14)	0	0.0382(13)	0

Table 4
Selected interatomic distances and BV values

Atom1	Atom2	Distance (Å)	BV	Atom1	Atom2	Distance (Å)	BV
Sm1	2 × S1	2.975(2)	0.317	Ti1	1 × S1	2.890(3)	0.173
Sm1	2 × S2	2.887 (4)	0.402	Ti1	1 × O1	1.911(9)	0.771
Sm1	2 × O1	2.380(5)	0.454	Ti1	2 × O3	1.927(2)	0.739
Sm1	1 × O1	2.423(5)	0.399	Ti1	1 × O4	1.829(9)	0.963
Sm1	1 × O3	2.552(9)	0.285	Ti1	1 × O4	2.130(7)	0.427
Sm1	1 × O5	2.538(12)	0.296/2				∑ = 3.83
			∑av. = 3.18				
				Ti2	2 × S1	2.613(2)	0.365
				Ti2	2 × S2	2.546(2)	0.437
Sm2	2 × S1	3.011(3)	0.288	Ti2	1 × O2	1.887(8)	0.771
Sm2	1 × S2	2.918(5)	0.370	Ti2	1 × O5	1.908(14)	0.729
Sm2	2 × O2	2.335(3)	0.513			1.87(2)	0.808
Sm2	1 × O2	2.427(7)	0.400				∑av. = 3.14
Sm2	1 × O3	2.622(5)	0.236				
Sm2	2 × O4	2.506(4)	0.323	Ti1	Ti1	3.014(3)	
			∑ = 3.25				

for sulfur atoms, the reliability factors converged to $R(\text{obs}) = 3.33\%$ and $R_w(\text{obs}) = 3.40\%$, for 1121 reflections ($I > 2\sigma(I)$) and 53 parameters. The final difference-Fourier map was featureless with the largest residuals +2.63 and −2.91 e Å^{-3}. Fractional coordinates and equivalent isotropic displacement parameters are listed in Table 2; anisotropic coefficients are reported in Table 3. Table 4 summarizes selected bond distances.

4. Description of the structure

The projection of the structure onto the (***a***,***c***) plane is shown on the Fig. 1 on which the atom labels correspond to those listed in Table 2. The structure is built up from double chains of Ti-centered octahedra between which Sm polyhedra develop (see Fig. 2).

Two kinds of double chains of Ti-centered octahedra are present. Along the ***c***-axis, these double chains are

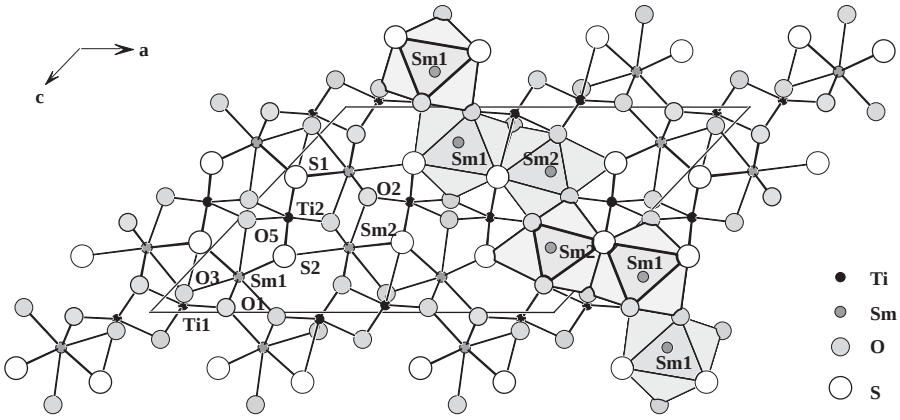

Fig. 1. Projection of the structure onto the $(\boldsymbol{a},\boldsymbol{c})$ plane. Polyhedral representation of the Sm-centered zig–zag chain is indicated.

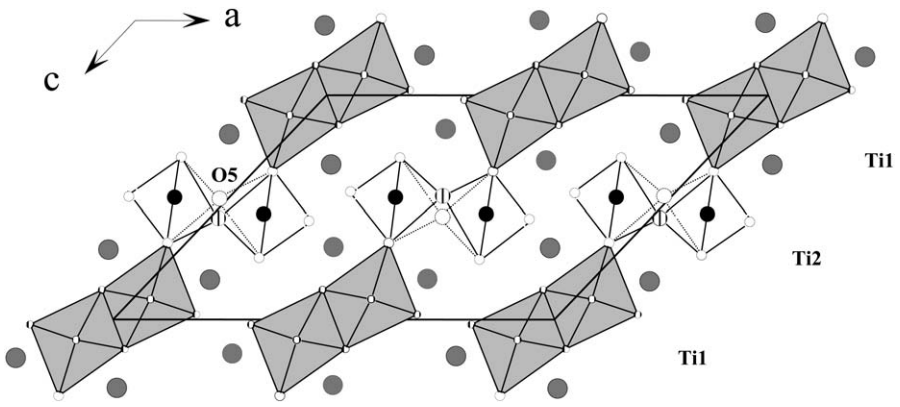

Fig. 2. Double chains of Ti-centered octahedra. For Ti1 the octahedra are shaded while for Ti2 they are opened.

connected via a S-atom corner (S1). For Ti1, the double chain is formed by edge-sharing octahedra in the $(\boldsymbol{a},\boldsymbol{c})$ plane and develops along the $\boldsymbol{b}$-axis through a common O corner (O3). On the contrary, the Ti2-centered octahedra share the O5 corner (split position) in the $(\boldsymbol{a},\boldsymbol{c})$ plane. These Ti2-centered octahedra form an edge-sharing infinite chain along the $\boldsymbol{b}$-axis (see Fig. 2). Because of the statistical distribution over two O5 sites, Sm1 is either 8 or 9 coordinated (bi- or tri-capped trigonal prisms). Sm-centered bi or tricapped trigonal prisms (Figs. 3a and b) encircle these chains. In the $(\boldsymbol{a}+\boldsymbol{c})$ direction, all Sm-centered polyhedra (shaded) are associated by sharing a triangular face and form a zig-zag chain (see Fig. 1).

All Ti-octahedra are distorted due to the mixed anion coordination (Fig. 3c and d). Ti1 octahedron is particularly distorted because of a single very long Ti–S distance ($d = 2.89$ Å). A Ti1–Ti1 distance of 3.014 Å is observed in the $(\boldsymbol{a},\boldsymbol{c})$ plane. The Ti2-compressed octahedron exhibits four S atoms in the rectangular plane and two O atoms in apical positions with smaller bond distances. One of them, namely O5, occupies a split position. The metal atom coordination and the main interatomic distances are indicated in Fig. 3.

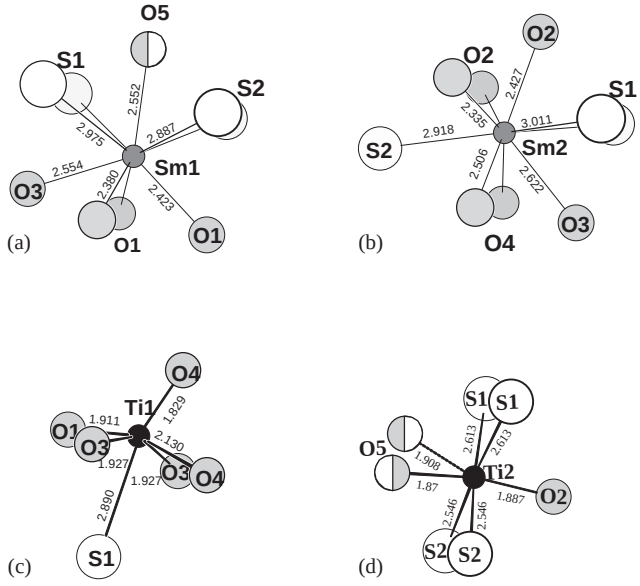

Fig. 3. Detailed environments around the different cations (a), (b) surroundings of Sm atoms (tricapped prism), (c) Ti1-octahedron showing the long Ti–S distance and (d) Ti2-centered octahedron. The split position (O5) is indicated.

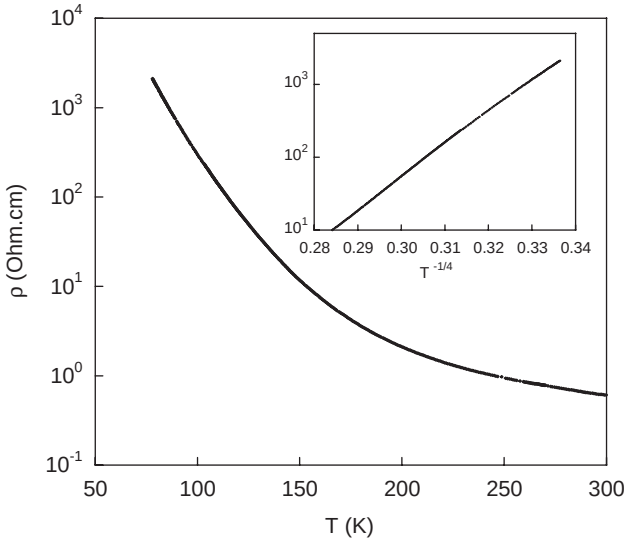

Fig. 4. Experimental resistivity versus temperature measured for $Sm_2Ti_2S_2O_{4.5}$. The inset shows the linear variation of the logarithm of the resistivity with $T^{-1/4}$.

5. Resistivity measurements

The DC resistivity of a needle like crystal of $Sm_2Ti_2S_2O_{4.5}$ was measured, along the ***b***-axis, between 297 and 77 K using a classical four probes configuration. As shown in Fig. 4 the measured resistivity shows a non-metallic behavior. However, the resistivity does not follow a simple activation law as expected for a normal semiconductor, with band gap energy lying between occupied and empty states. On the contrary, at low temperature (<150 K), the resistivity, plotted in logarithmic scale, seems to vary linearly with $T^{-1/4}$ which could indicate a variable range hopping behavior (see inset of Fig. 4).

6. Discussion and concluding remarks

$Sm_2Ti_2S_2O_{4.5}$ has a formulation very close to that of the defect Ruddelsden–Popper phase $Sm_2Ti_2S_2O_5$. Surprisingly, both compounds do not differ because of an oxygen non-stoichiometry as often observed in the Ruddelsden–Popper oxides, but exhibit very different structures. For $Sm_2Ti_2S_2O_5$, the titanium atoms are all found at the +IV oxidation state, and occupy a distorted octahedron made of five oxygen atoms and one sulfur atom. For $Sm_2Ti_2S_2O_{4.5}$, the situation is quite different. First, owing to the absence of short anion–anion bonding, the oxidation state equilibrium is only satisfied with Ti cations at the +III and +IV oxidation state, in a 1/1 ratio. Bond valence (BV) calculations [14] fully corroborate this assumption, and clearly assign the +IV oxidation state to Ti1, and the +III oxidation state to Ti2 (see Table 4). This result has to be pointed out, as it is rather rare to distinguish Ti(+III) from Ti(+IV) over the non-equivalent crystallographic sites. Among the reported mixed valent titanium quaternary oxychalcogenides, this was only possible for $La_6Ti_3Se_9O_5$ [7]. A careful examination of the anion coordination as well as Ti–O/Se distances within the different Ti-octahedra, leads the authors to distinguish between the Ti(+III) and Ti(+IV) sites, and this choice was rather confirmed by BV calculations. For $Sm_2Ti_2S_2O_{4.5}$, assigning Ti(+III) and Ti(+IV) regarding the more oxidizing character of O compared to S is also possible. In this compound, the Ti(+IV) species (=Ti1) are surrounded by five O atoms and one S atom, while the Ti(+III) species (=Ti2) are coordinated by four S atoms and two O atoms. It is worth noting that for both compounds $Sm_2Ti_2S_2O_{4.5}$ and $Sm_2Ti_2S_2O_5$, the Ti (+IV) atoms adopt similar octahedral coordination with five oxygen atoms and one sulfur atom. Finally, the difference between the structures of $Sm_2Ti_2S_2O_{4.5}$ and $Sm_2Ti_2S_2O_5$ is related to the anionic environment observed between Ti(+III) and Ti(+IV).

In the compound $Sm_2Ti_2S_2O_{4.5}$, the Ti(+III) atoms (i.e. Ti2 atoms with a d^1 configuration in a sulfur rich environment) form 1D chains of edge sharing octahedron. According to the usual octahedral crystal field splitting, the T_{2g} band of titanium should be incompletely filled and therefore a metallic character should appear along the chain. Indeed, $LiTiS_2$ that contains titanium atoms with a d^1 configuration and exhibits a partially filled T_{2g} band, is a metallic compound. However the resistivity measurement performed for $Sm_2Ti_2S_2O_{4.5}$ shows a non-metallic behavior, which means that the electrons are not delocalized along the chains. With Ti–Ti distances of about 3.45 Å the electron delocalization is possible in $LiTiS_2$. Likely for $Sm_2Ti_2S_2O_{4.5}$ the longer Ti–Ti distance observed along the chain (3.716 Å) prevents any electron delocalization and the appearance of a metallic character.

Acknowledgments

B. Corraze is thanked for his help in performing DC conductivity measurements.

References

[1] K. Ueda, S. Inoue, H. Hosono, N. Sarukura, M. Hirano, Appl. Phys. Lett. 78 (2001) 2333–2335.
[2] (a) A. Ishikawa, T. Takata, J.N. Kondo, M. Hara, H. Kobayashi, K. Domen, J. Am. Chem. Soc. 124 (2002) 13547–13553;
(b) A. Ishikawa, Y. Yamada, T. Takata, J.N. Kondo, M. Hara, H. Kobayashi, K. Domen, Chem. Mater. 15 (2003) 4442–4446.

[3] V. Meignen, L. Cario, A. Lafond, Y. Moëlo, C. Guillot-Deudon, A. Meerschaut, J. Solid State Chem. (2003), accepted.
[4] W.J. Zhu, P.H. Hor, J. Solid State Chem. 134 (1997) 128–131.
[5] K. Otzschi, H. Ogino, J.I. Shimoyama, K. Kishio, J. Low Temp. Phys. 117 (1999) 729–733.
[6] (a) L. Cario, C. Deudon, A. Meerschaut, J. Rouxel, J. Solid State Chem. 136 (1998) 46–50;
(b) L.J. Tranchitella, J.C. Fettinger, S.F. Heller-Zeisler, B.W. Eichhorn, Chem. Mater. 10 (1998) 2078–2085.
[7] O. Tougait, J. Ibers, J. Solid State Chem. 157 (2001) 289–295.
[8] (a) C. Boyer, C. Deudon, A. Meerschaut, C. R. Acad. Sci., t.2, Série IIc (1999) 93–99;
(b) M. Goga, R. Seshadri, V. Ksenofontov, P. Gütlich, W. Tremel, Chem. Commun. (1999) 979–980.
[9] A. Meerschaut, A. Lafond, V. Meignen, C. Deudon, J. Solid State Chem. 162 (2001) 182–187.
[10] S.G. Denis, S.J. Clarke, Chem. Commun. (2001) 2356–2357.
[11] Nonius (1997–2001), COLLECT, Nonius BV, Delft, The Netherlands.
[12] G.M. Sheldrick, SHELXS97, University of Göttingen, Germany, 1997.
[13] V. Petricek, M. Dusek, JANA2000, Institute of Physics, Praha, Czech Republic, 2000.
[14] N.E. Brese, M. O'Keeffe, Acta Cryst. B47 (1991) 192–197.